Theory of magnetoelectric effects in ferrite piezoelectric nanocomposites

V. M. Petrov and G. Srinivasan
Physics Department, Oakland University, Rochester, Michigan 48309, USA

M. I. Bichurin
Institute of Electronic Information Systems, Novgorod State University, B. S. Peterburgskaya St. 41, 173003 Veliky Novgorod, Russia

A. Gupta
Center for Materials for Information Technology, University of Alabama, Tuscaloosa, Alabama 35487, USA
(Received 2 January 2007; revised manuscript received 30 March 2007; published 8 June 2007)

A model is presented for low-frequency magnetoelectric (ME) effects in nanobilayers, nanopillars, and nanowires of nickel ferrite (NFO) and lead zirconate titanate (PZT) on MgO substrates or templates. The clamping effect of the substrate for the bilayer and pillars and of the template for the wires have been considered in determining the ME voltage coefficient. The ME interactions have been found to be the strongest for field orientations corresponding to minimum demagnetizing fields, i.e., in-plane fields for bilayers and axial fields for pillars and wires. It is shown that the coupling strength decreases with increasing substrate clamping. For increasing volume of MgO substrate in a bilayer, (i) the ME coefficient drops exponentially and (ii) the PZT volume required for maximum ME effects increases. For nanopillars of NFO in PZT matrix on MgO, the substrate pinning effects are negligible only when the length of the pillar is much greater than its radius. In the case of NFO-PZT nanowires grown on a MgO nanowire template, the ME coefficient is predicted to decrease from a maximum to approaching zero as the radius of the template layer is increased.

DOI: 10.1103/PhysRevB.75.224407 PACS number(s): 75.80.+q, 77.65.−j, 77.84.−s, 75.75.+a

Materials in which ferromagnetism and ferroelectricity occur simultaneously in the same phase and allow coupling between the two are known as magnetoelectric (ME) multiferroics. Most of the known single-phase ME materials show weak ME coupling.[1–3] Relatively large ME coefficients, however, have been obtained in layered composites consisting of piezoelectric and magnetostrictive materials.[4–11] When a magnetic field is applied to the composites, the magnetostrictive phase induces a strain in terms of a shape change, which in turn exerts stress on the piezoelectric phase, resulting in an electric polarization. Lead zirconate titanate (PZT)-ferrite and PZT-Terfenol-D are the most studied composites to date.[10–12] One of largest ME voltage coefficients of 500 V cm^{-1} Oe^{-1} was reported recently for a high permeability magnetostrictive piezofiber laminate.[13]

Nanostructures in the shape of wires, pillars, and films are important for increased functionality in miniature devices. The multiferroic composites can be created in three forms: (a) alternate layers of piezoelectric and magnetostrictive materials, (b) nanopillars of magnetostrictive material in a piezoelectric matrix, and (c) nanowires of ferrite and PZT on a template. The ME coupling in two-dimensional structures such as thin films is expected to be weak due to the strong substrate clamping effect. In a significant development, it has been demonstrated that the issue of substrate clamping can be avoided by fabricating self-assembled ferrite, such as cobalt ferrite, in a ferroelectric matrix to enhance the ME coupling.[14] Nan *et al.*[15] modeled the static ME effects in $BaTiO_3$-$CoFe_2O_4$ nanopillars and nanobilayers. They considered the effects of residual strain on polarization and the effect of ME interactions on induced polarization using the Landau-Ginsberg-Devonshire theory. The model predicted a ferroelectric-ferromagnetic coupling in the nanopillars that is much stronger than in bulk counterparts or in nanobilayers.

Similarly, one-dimensional (1D) nanostructures such as nanowires, nanotubes, nanorods, etc., constitute an important class of materials that are presently a subject of very active investigation.[16,17] Because of the large surface areas of 1D nanostructures, a more effective interface coupling and an enhancement in the ME effect are expected. A fundamental understanding of the size- and shape-dependent scaling behavior of the ME effect in composites, particularly down to nanoscale dimensions, is presently lacking. An improved knowledge of the nanoscale ME properties will help achieve miniaturization of potential magnetoelectric devices.

This work is focused on modeling the ME effects in ferrite piezoelectric nanobilayers, nanopillars, and nanowires. We have chosen nickel ferrite (NFO)-PZT grown on MgO substrates or templates as the model system. Experiments on thick film NFO-PZT bilayers have revealed a giant ME coupling in the low-frequency region.[10] We have selected MgO as the bilayer substrate and nanowire template because of its chemical inertness. Additionally, vertical arrays of single-crystalline MgO nanowires can be readily grown using a simple vapor deposition technique,[18] which can be used as a template to produce the nanowire ME structures discussed in this paper. Further, it can be synthesized quite readily and is closely lattice matched with our chosen ferromagnetic-ferroelectric oxides. The MgO crystal has the rocksalt structure with a lattice parameter of 0.4213 nm. Nickel ferrite ($NiFe_2O_4$) has the inverse spinel structure with cubic lattice parameters of 0.8340 nm, almost exactly double of MgO (lattice mismatch of −1.02%,). This makes MgO a convenient substrate and/or template from a lattice matching point of view. $NiFe_2O_4$ has excellent magnetomechanical coupling, in the ferrite family. Both $BaTiO_3$ and $Pb(Zr_{1-x}Ti_x)O_3$ are well-known ferroelectric oxides with a distorted perovskite structure, which also have large piezoelectric coefficients. The lattice mismatch between MgO and $BaTiO_3$ (tetragonal lattice, $a=0.3992$ nm, $c=0.4036$ nm) is quite large

(−5.3% and −4.2%, respectively). Nevertheless, epitaxial films of $BaTiO_3$ can be readily grown on MgO substrates using various methods.[18] The mismatch PZT and MgO is also large, although it is somewhat smaller than with BTO [for $Pb(Zr_{0.52}Ti_{0.48})O_3$, $a=b=0.403$ nm, $c=0.414$ nm].

In this work, the ME voltage coefficients α_E have been estimated for field orientations corresponding to minimum demagnetizing fields and maximum α_E. The effect of substrate or template clamping has been described in terms of dependence of α_E on substrate and/or template dimensions or volume fraction. In the case of bilayers, α_E drops exponentially with increasing volume of MgO. For nanopillars of NFO in PZT matrix, the substrate pinning effects are negligible as long as the length of the pillar is much greater than its radius. For NFO-PZT nanowires on MgO templates, the ME coefficient is predicted to decrease from a maximum to approaching zero as the radius of the template is increased.

For the estimation of α_E it is assumed that the piezoelectric phase is electrically poled in a dc field E and that the composite is subjected to a bias field H and an ac magnetic field δH, giving rise to a piezomagnetic deformation. We then solve magnetostatic and elastostatic equations in NFO, and elastostatic and electrostatic equations in PZT, taking into account boundary conditions. The nanocomposite is considered as a homogeneous medium for determining the ME susceptibility from the effective material parameters that relate the stress-strain and electric and magnetic fields and inductions.[19,20] Then, the ME voltage coefficient, which is the ratio of ME susceptibility and permittivity, is calculated. The model can be used to estimate the ME couplings from known material parameters (piezoelectric coefficients, magnetostriction, stiffness, etc.) or data on ME coupling can be used to extract composite parameters.

For a polarized piezoelectric phase with the symmetry ∞m and magnetostrictive phase with cubic symmetry, the following equations can be written for the strain and electric and magnetic displacements:

$$
\begin{aligned}
{}^{p}S_i &= {}^{p}s_{ij}\,{}^{p}T_j + {}^{p}d_{ki}\,{}^{p}E_k,\\
{}^{p}D_k &= {}^{p}d_{ki}\,{}^{p}T_i + {}^{p}\varepsilon_{kn}\,{}^{p}E_n,\\
{}^{m}S_i &= {}^{m}s_{ij}\,{}^{m}T_j + {}^{m}q_{ki}\,{}^{m}H_k,\\
{}^{m}B_k &= {}^{m}q_{ki}\,{}^{m}T_i + {}^{m}\mu_{kn}\,{}^{m}H_n,\\
{}^{s}S_i &= {}^{s}s_{ij}\,{}^{s}T_j,
\end{aligned}
\qquad (1)
$$

where S_i and T_j are strain and stress tensor components, E_k and D_k are the vector components of electric field and electric displacement, H_k and B_k are the vector components of magnetic field and magnetic induction, s_{ij}, q_{ki}, and d_{ki} are compliance, piezomagnetic, and piezoelectric coefficients, ε_{kn} is the permittivity matrix, and μ_{kn} is the permeability matrix. The superscripts p, m, and s correspond to piezoelectric and piezomagnetic phases and substrate or nanowire template, respectively.

Next, the nanocomposite is considered as homogeneous and the average S_i, T_j, E_k, H_k, D_k, and B_k are given by

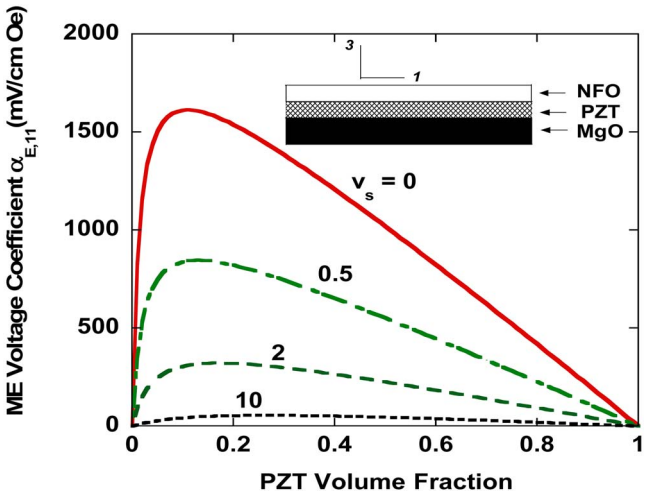

FIG. 1. (Color online) Diagram showing a nickel ferrite (NFO)-lead zirconate titanate (PZT) nanobilayer in the (1,2) plane on MgO substrate. It is assumed that PZT is poled with an electric field E_1 along 1, the bias magnetic field H_1 and ac magnetic field δH_1 are along axis 1, and the ac electric field δE_1 is measured along direction 1. Estimated PZT volume fraction dependence of in-plane longitudinal ME voltage coefficient $\alpha_{E,11}=\delta E_1/\delta H_1$ is shown for a series of volume fraction v_s for MgO.

$$
\begin{aligned}
S_i &= s_{ij}T_j + d_{ki}E_k + q_{ki}H_k,\\
D_k &= d_{ki}T_i + \varepsilon_{kn}E_n + m_{kn}H_n,\\
B_k &= q_{ki}T_i + m_{kn}E_n + \mu_{kn}H_n,
\end{aligned}
\qquad (2)
$$

where s_{ij}, d_{ki}, and q_{ki} are effective compliance, piezoelectric, and piezomagnetic coefficients, and ε_{kn}, μ_{kn}, and m_{kn} are effective permittivity, permeability, and ME coefficient. Solving Eqs. (2) and taking into account the solutions of Eqs. (1), all effective parameters appearing in Eq. (2) can be obtained.

ME effects in a nanobilayer. The ME coupling in a nanobilayer of NFO-PZT on MgO substrate is considered first. In our earlier modeling efforts on a ferrite-PZT layered system, it was shown that α_E is expected to be maximum for in-plane longitudinal fields; i.e., the dc bias magnetic field and the ac electric and magnetic field are all parallel to each other and to the sample plane.[19,20] For the two other field orientations, out-of-plane longitudinal and in-plane transverse fields, α_E is predicted to be weak due to combination of weak piezomagnetic and piezoelectric couplings and demagnetizing fields.[20] These predictions are in general agreement with data.[9–12] Thus, the estimates of α_E here for a NFO-PZT bilayer on MgO are limited to in-plane longitudinal fields. We assume a coordinate system with the sample in the (1,2) plane, as in Fig. 1, and that the piezoelectric phase is poled with an electric field E along direction 1 and that a bias magnetic field H_1 and an ac field δH_1 are applied along the same direction (direction 1). The resulting ac electric field is measured along the same direction for the determination of the ME voltage coefficient $\alpha_{E11}=\delta E_1/\delta H_1$. For the solution of the set of Eqs. (1) and (2), the following boundary conditions are used:

TABLE I. Material parameters (compliance coefficient s, piezomagnetic coupling q, piezoelectric coefficient d, and permittivity ε) for nickel ferrite (NFO) and lead zirconate titanate (PZT) used for theoretical estimates (Refs. 24 and 25).

Material	s_{11} (10^{-12} m^2/N)	s_{12} (10^{-12} m^2/N)	q_{11} (10^{-12} m/A)	q_{12} (10^{-12} m/A)	d_{12} (10^{-12} m/V)	d_{11} (10^{-12} m/V)	$\varepsilon_{33}/\varepsilon_0$
PZT	17.3	−7.22			−175	400	1750
NFO	6.5	−2.4	−680	125			10
MgO	4	0.96					9.6

$$
{}^{p}S_1 = {}^{m}S_1 = {}^{s}S_1,
$$

$$
{}^{p}S_2 = {}^{m}S_2 = {}^{s}S_2,
$$

$$
{}^{p}T_1 v + {}^{m}T_1(1-v) + {}^{s}T_1 v_s = 0,
$$

$$
{}^{p}T_2 v + {}^{m}T_2(1-v) + {}^{s}T_2 v_s = 0, \tag{3}
$$

where $v = {}^{p}v/({}^{p}v + {}^{m}v)$, $v_s = {}^{s}v/({}^{p}v + {}^{m}v)$, and ${}^{p}v$, ${}^{m}v$, and ${}^{s}v$ denote the volume of piezoelectric and magnetostrictive phases and substrate, respectively. The third and fourth terms in Eq. (3) correspond to equilibrium condition (the total force projections on 1 and 2 axes are equal to zero). Originally the cross-sectional areas must enter these equations. Since the sizes of all layers in 1 and 2 axes are equal, the cross-sectional areas are replaced by volumes.

We assume here that the strains of NFO and PZT match at the interface. However, this will not be the case if there is strain relaxation due to dislocation or other defects. Strain relaxation in heteroepitaxial systems, a subject of several theoretical studies, can result from lattice mismatch of film and substrate. For heteroepitaxial growth of a film, the lattice mismatch can be taken into account on the basis of the Green's function formalism.[21] This approach makes use of the analytical expression for the half-space Green's function that describes the displacement at any point x in the bulk due to a unit force acting at another point x'. Assuming that the bulk is homogeneously strained, a multipole expansion of the force distribution caused by a step on a strained vicinal surface can be made. Multiplying each term in the expansion by the appropriate derivative of the Green's function, the displacement at any point due to the presence of a step can be obtained as well as the force on one step due to another. However, the use of the half-space Green's function implies not only that the epilayer is homogeneously strained but also that the epilayer thickness is much greater than the step height. A more complete approach for taking into account the strain relaxation is based on lattice statistics using linear elasticity theory.[22,23] According to this theory, the description of the strain relaxation is carried out by minimizing the free energy of epitaxial system. Since the elastic energy depends on lattice mismatch, the heteroepitaxial growth of a film with a lattice constant a_f on a substrate with a lattice constant a_s is equal to $(a_f - a_s)/a_s$. Then, one has to solve the problem of step relaxations and step-step interactions on vicinal surfaces. Estimates showed that for small lattice mismatch and epilayer heights of roughly 30–50 monolayers, the effects of the substrate could be quite weak. In our calculations, we suppose that epilayer thickness is sufficiently large to neglect the influence of strain relaxation on average stresses in the structures that determine the ME voltage coefficient.

The ME voltage coefficient is calculated numerically from Eqs. (1)–(3) and using the open circuit condition $D_1 = 0$.[20] Figure 1 shows the PZT volume fraction dependence of ME voltage coefficient for NFO-PZT on MgO that is characterized by material parameters listed in Table I.[24,25] For a freestanding nanobilayer, $\alpha_{E,11}$ increases with increasing PZT volume, attains a peak value of 1.6 V/cm Oe for $v = 0.11$, and then drops rapidly with increasing v. Pure PZT ($v=1$) and pure NFO ($v=0$) do not reveal the ME effect. Therefore, the ME voltage coefficient has maximum as a function of PZT volume fraction. The peak in the ME voltage coefficient is displaced toward the low value of PZT volume fraction since the ME voltage coefficient equals to ratio of ME susceptibility to permittivity. The ME susceptibility has maximum at about $v \approx 0.5$ and permittivity monotonically increases with PZT volume fraction. This results in displacement of the peak toward the low value of PZT volume fraction

A dramatic, factor-of-2 decrease in $\alpha_{E,11}$ is expected when the film is deposited on a thin MgO substrate of volume that is only 50% of the film volume. As seen in Fig. 1, further increase in v_s leads to a substantial decrease in $\alpha_{E,11}$ and the ME coupling vanishes when the film is assumed to be on MgO of volume fraction 10 or more. Figure 2 shows the variation in the peak value of $\alpha_{E,11}$ with the substrate volume

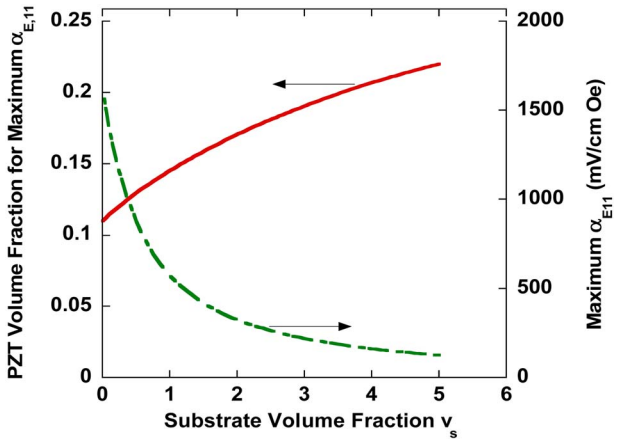

FIG. 2. (Color online) Variation with substrate volume fraction v_s of the peak value of ME voltage coefficient $\alpha_{E,11}$ in Fig. 1 and the corresponding PZT volume fraction.

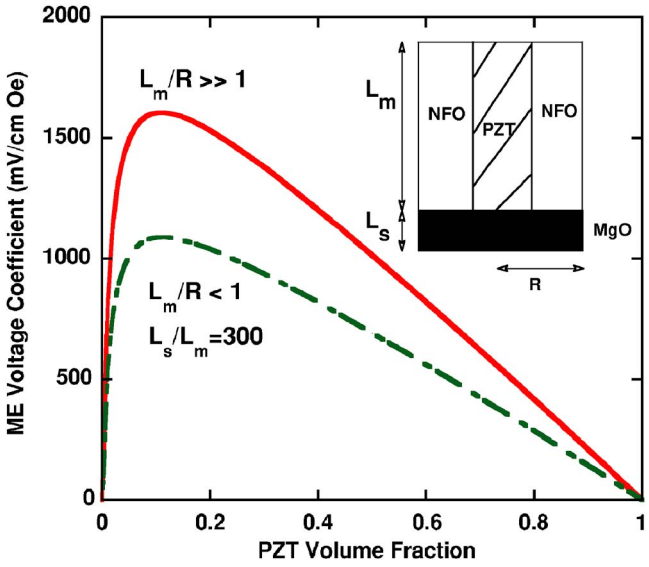

FIG. 3. (Color online) A nanopillar of NFO and PZT of radius R and length L_m on an MgO substrate of thickness L_s. All the electric and magnetic fields are assumed to be along the axis (direction 3) of the pillars. Estimated PZT volume fraction dependence of ME voltage coefficient $\alpha_{E,33}$ for NFO-PZT nanopillar is shown.

fraction v_s along with the PZT volume fraction v corresponding to peak $\alpha_{E,11}$. The upshift of the PZT volume fraction that results in maximal ME effect is stipulated by variation of effective compliance of the sample with the substrate thickness.

ME effect in a nanopillar. Multilayer heterostructures with piezoelectric and magnetostrictive layers in the form of nanopillars can mimic the functionality of a "true" single-phase multiferroic materials. However, it is clear from the results in Figs. 1 and 2 that magnetoelectric properties of mechanically coupled bilayer will be adversely affected by substrate clamping. Therefore, as an alternative, we have modeled nanopillars of NFO grown in a PZT matrix. Such heterostructures can still be limited by clamping due to the substrate on which they are grown. Zheng *et al.*[14] have demonstrated nanopillars of $CoFe_2O_4$ in $BaTiO_3$ matrix by pulsed laser deposition on (001) $SrTiO_3$ substrates. We consider here a nanopillar of NFO and PZT. The unit of this structure can be modeled by two coaxial cylinders consisting of ferrite and PZT on MgO, as in Fig. 3. In terms of mechanical connectivity, such a structure is also known as a 3-1 composite since the ferrite has continuity in all three axes whereas PZT connectivity is limited to only one axis. Directions of polarization and ac electric and ac and dc magnetic fields are supposed to coincide with the axis of the cylinders. Taking into account the axial symmetry, the elastostatic equation for this case is written in cylindrical coordinates,

$$\frac{\partial T_{rr}}{\partial r} + \frac{1}{r}(T_{rr} - T_{\theta\theta}) = 0. \tag{4}$$

Transferring Eqs. (2) to cylindrical coordinates by means of tensor relations,[26] one finds

$$^{m}S_{rr} = {}^{m}s_{11}\,{}^{m}T_{rr} + {}^{m}s_{12}\,{}^{m}T_{\theta\theta} + {}^{m}s_{12}\,{}^{m}T_{zz} + {}^{m}q_{31}H_3,$$

$$^{m}S_{\theta\theta} = {}^{m}s_{12}\,{}^{m}T_{rr} + {}^{m}s_{11}\,{}^{m}T_{\theta\theta} + {}^{m}s_{12}\,{}^{m}T_{zz} + {}^{m}q_{31}H_3,$$

$$^{m}S_{zz} = {}^{m}s_{12}({}^{m}T_{rr} + {}^{m}T_{\theta\theta}) + {}^{m}s_{11}\,{}^{m}T_{zz} + {}^{m}q_{33}H_3,$$

$$^{p}S_{rr} = {}^{p}s_{11}\,{}^{p}T_{rr} + {}^{p}s_{12}\,{}^{p}T_{\theta\theta} + {}^{p}s_{13}\,{}^{p}T_{zz} + {}^{p}d_{31}E_3,$$

$$^{p}S_{\theta\theta} = {}^{p}s_{12}\,{}^{p}T_{rr} + {}^{p}s_{11}\,{}^{p}T_{\theta\theta} + {}^{p}s_{13}\,{}^{p}T_{zz} + {}^{p}d_{31}E_3,$$

$$^{p}S_{zz} = {}^{p}s_{13}({}^{p}T_{rr} + {}^{p}T_{\theta\theta}) + {}^{p}s_{33}\,{}^{p}T_{zz} + {}^{p}d_{33}E_3,$$

$$^{p}D_3 = {}^{p}d_{31}({}^{p}T_{rr} + {}^{p}T_{\theta\theta}) + {}^{p}d_{33}\,{}^{p}T_{zz} + {}^{p}\varepsilon_{33}E_3. \tag{5}$$

Similar equations can be written for MgO substrate:

$$^{s}S_{rr} = {}^{s}s_{11}\,{}^{s}T_{rr} + {}^{s}s_{12}\,{}^{s}T_{\theta\theta} + {}^{s}s_{13}\,{}^{s}T_{zz},$$

$$^{s}S_{\theta\theta} = {}^{s}s_{12}\,{}^{s}T_{rr} + {}^{s}s_{11}\,{}^{s}T_{\theta\theta} + {}^{s}s_{13}\,{}^{s}T_{zz}.$$

Expressing the stress tensor component by strain tensor component from Eqs. (5) and substituting into Eq. (4), the following equation can be obtained for the radial displacement u_r that defines strain components $S_{rr} = \partial u_r/\partial r$ and $S_{\theta\theta} = u_r/r$ for both phases and MgO substrate:

$$\frac{\partial^2 u_r}{\partial r^2} + \frac{1}{r}\frac{\partial u_r}{\partial r} - \frac{u_r}{r^2} = 0. \tag{6}$$

The boundary conditions in this case have the form

$$^{m}T_r = 0 \quad \text{at} \quad r = {}^{m}R,$$

$$^{p}S_{zz} = {}^{m}S_{zz},$$

$$^{p}u_r = {}^{s}u_r = 0 \quad \text{at} \quad r = 0,$$

$$^{p}u_r = {}^{m}u_r \quad \text{at} \quad r = {}^{p}R,$$

$$^{p}T_r = {}^{m}T_r \quad \text{at} \quad r = {}^{p}R,$$

$$^{m}T_r L_m = -\,{}^{s}T_r L_s \quad \text{for} \quad L_m/R < 1 \quad \text{and} \quad {}^{m}T_r = 0 \quad \text{for} \quad L_m/R \gg 1 \quad \text{at} \quad r = {}^{m}R,$$

$$^{s}u_r = {}^{m}u_r \quad \text{for} \quad L_m/R < 1 \quad \text{at} \quad r = {}^{s}R, \tag{7}$$

where ${}^{p}R$ and ${}^{m}R$ are radii of piezoelectric and piezomagnetic phases with $R={}^{m}R$.

Strains and stresses in the z direction are determined by following expressions:

$$ {}^{p}S_{zz} = {}^{m}S_{zz}, $$

$$ \int_{0}^{{}^{p}R} {}^{p}T_{zz} r dr = -\int_{{}^{p}R}^{{}^{m}R} {}^{m}T_{zz} r dr. \tag{8} $$

Equations (5)–(8) and open circuit condition $D_3=0$ constitute a closed system and can be numerically solved for the ME voltage coefficient $\alpha_{E,33}$. Numerical computation results are shown in Fig. 3 for NFO-PZT pillars on MgO.

Results in Fig. 3 indicate no clamping due to MgO when the length of the pillar L_m is greater than its radius R. The magnitude of $\alpha_{E,33}$ and its variation with PZT volume fraction v are similar to those of in-plane ME interactions in a freestanding bilayer (Fig. 1). For the nanopillar, substrate clamping and demagnetization effects become important only when $L_m < R$ and substrate thickness $L_s \gg L_m$, leading to a substantial reduction in $\alpha_{E,33}$.

It is appropriate here to compare the results in Fig. 3 with the model discussed in Ref. 15 for static ME effects in $CoFe_2O_4$-$BaTiO_3$ nanopillars that was based on the Green's function approach. The model compared the estimates on ME coupling in bulk composites, bilayers, and nanopillars of the ferrite in barium titanate matrix. It accounted for the experimentally observed magnetic-field induced polarization[14] that was attributed to the enhancement in the elastic coupling. Our results in Fig. 3 also predict strong ME coupling in nanopillars that will not be influenced by the substrate coupling when the pillar height is much greater than its radius, in agreement with the results in Ref. 15.

ME effect in a nanowire. Finally, we now consider a nanowire geometry for the ferrite-PZT grown on a MgO template as shown in Fig. 4. The ME voltage coefficient can be found in this case similar to the case of the nanopillar geometry. However, we must add three supplementary equations to Eq. (5) to account for the presence of the MgO template:

$$ {}^{s}S_{rr} = {}^{s}s_{11}\,{}^{s}T_{rr} + {}^{s}s_{12}\,{}^{s}T_{\theta\theta} + {}^{s}s_{13}\,{}^{s}T_{zz}, $$

$$ {}^{s}S_{\theta\theta} = {}^{s}s_{12}\,{}^{s}T_{rr} + {}^{s}s_{11}\,{}^{s}T_{\theta\theta} + {}^{s}s_{13}\,{}^{s}T_{zz}, $$

$$ {}^{s}S_{zz} = {}^{s}s_{12}({}^{s}T_{rr} + {}^{s}T_{\theta\theta}) + {}^{s}s_{11}\,{}^{s}T_{zz}. \tag{9} $$

The boundary conditions in this case take the form

$$ {}^{s}u_r = 0 \quad \text{at} \quad r = 0, $$

$$ {}^{s}u_r = {}^{m}u_r \quad \text{at} \quad r = {}^{s}R, $$

$$ {}^{s}T_r = {}^{m}T_r \quad \text{at} \quad r = {}^{s}R, $$

$$ {}^{p}u_r = {}^{m}u_r \quad \text{at} \quad r = {}^{m}R, $$

$$ {}^{p}T_r = {}^{m}T_r \quad \text{at} \quad r = {}^{m}R, $$

$$ {}^{p}T_r = 0 \quad \text{at} \quad r = {}^{p}R, $$

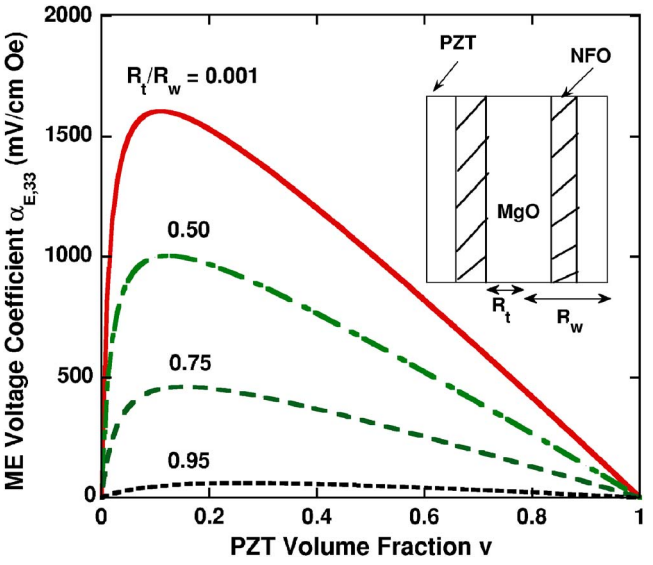

FIG. 4. (Color online) Nanowire structure of NFO-PZT grown on an MgO template. The poling fields and the ac and dc fields are assumed to be along the axis (direction 3). Estimated PZT volume fraction dependence of ME voltage coefficient $\alpha_{E,33}$ is shown for a series of ratio of template radius R_t to wire radius R_w.

$$ {}^{p}S_{zz} = {}^{m}S_{zz} = {}^{s}S_{zz}, $$

$$ \int_{{}^{m}R}^{{}^{p}R} {}^{p}T_{zz} r dr + \int_{{}^{s}R}^{{}^{m}R} {}^{m}T_{zz} r dr + \int_{0}^{{}^{s}R} {}^{s}T_{zz} r dr = 0. \tag{10} $$

Equations (5)–(10) are solved numerically to obtain the PZT volume fraction dependence of the ME voltage coefficient $\alpha_{E,33}$, which is presented in Fig. 4. For a NFO-PZT sheath (wire without template), the variation of $\alpha_{E,33}$ with v is quantitatively similar to the case of substrate-free bilayer (Fig. 1) or a long and thin nanopillar (Fig. 3). An increase in the radius of MgO is predicted to decrease $\alpha_{E,33}$ by 40% when the template radius equals the combined thickness of NFO and PZT. Comparison of the strength of ME effects for wires and bilayers shows that for the wire, the radial stress is added to in-plane stresses. This results in stronger ME effects than for the bilayer.

In conclusion, a model has been developed for low-frequency ME interactions in ferrite-PZT nanostructures. Although the estimates here are based on bulk material parameters, it can easily be refined to take into account parameters for nanosized ferrites and PZT when they become available. For a NFO-PZT nanobilayer on MgO substrates, the strength of ME interactions is weaker than thick film bilayers due to the strong clamping effects of the substrate. Similarly, for nanowires on MgO templates, the template reduces the strength of ME effect, similar to the case of bilayers, but to a much smaller extent both because of the reduced volume and the addition of the radial and in-plane stresses. The strongest interactions, however, are expected for nickel ferrite nanopillars in a PZT matrix.

The work at Oakland University was supported by NSF

grants (NIRT-0609377 and ECS-0621907). The work at Novgorod State University was supported by the Russian Foundation for Basic Research (Projects No. 06-08-00896-a, No. 06-02-08071-ofi, and No. 05-02-39002-GFEN-a). The work at the University of Alabama was supported by the NSF Grant No. ECS-0621850.

[1] G. T. Rado and V. J. Folen, Phys. Rev. Lett. **7**, 310 (1961).
[2] E. Kita, S. Takano, A. Tasaki, K. Siratori, K. Kohn, and S. Kimura, J. Appl. Phys. **64**, 5659 (1988).
[3] J. Wang, J. B. Neaton, H. Zheng, V. Nagarajan, S. B. Ogale, B. Liu, D. Viehland, V. Vaithyanathan, D. G. Schlom, U. V. Waghmare, N. A. Spaldin, K. M. Rabe, M. Wuttig, and R. Ramesh, Science **299**, 1719 (2003).
[4] T. G. Lupeiko, I. V. Lisnevskaya, M. D. Chkheidze, and B. I. Zvyagintsev, Inorg. Mater. **31**, 1139 (1995).
[5] J. Ryu, A. V. Carazo, K. Uchino, and H. Kim, Jpn. J. Appl. Phys., Part 1 **40**, 4948 (2001).
[6] K. Mori and M. Wuttig, Appl. Phys. Lett. **81**, 100 (2002).
[7] S. Dong, J. F. Li, and D. Viehland, Philos. Mag. Lett. **83**, 769 (2003).
[8] N. Cai, C. W. Nan, J. Zhai, and Y. Lin, Appl. Phys. Lett. **84**, 3516 (2004).
[9] G. Srinivasan, E. T. Rasmussen, B. J. Levin, and R. Hayes, Phys. Rev. B **65**, 134402 (2002).
[10] G. Srinivasan, E. T. Rasmussen, J. Gallegos, R. Srinivasan, Yu. I. Bokhan, and V. M. Laletin, Phys. Rev. B **64**, 214408 (2001).
[11] G. Srinivasan, E. T. Rasmussen, and R. Hayes, Phys. Rev. B **67**, 014418 (2003).
[12] S. Dong, J. Zhai, F. Bai, J. F. Li, and D. Viehland, Appl. Phys. Lett. **87**, 062502 (2005).
[13] S. Dong, J. Zhai, J. Li, and, D. Viehland, Appl. Phys. Lett. **89**, 252904 (2006).
[14] H. Zheng, J. Wang, L. Mohaddes-Ardabili, M. Wuttig, L. Salamanca-Riba, D. G. Schlom, and R. Ramesh, Appl. Phys. Lett. **85**, 2035 (2004); H. Zheng *et al.*, Science **303**, 661 (2004).
[15] Ce-Wen Nan, G. Liu, Y. Lin, and H. Chen, Phys. Rev. Lett. **94**, 197203 (2005); G. Liu, Ce-Wen Nan, Z. K. Xu, and H. Chen, J. Phys. D **38**, 2321 (2005).
[16] M. Law, J. Goldberger, and P. Yang, Annu. Rev. Mater. Res. **34**, 83 (2004).
[17] Y. Xia, P. Yang, Y. Sun, Y. Wu, B. Mayers, B. Gates, Y. Yin, F. Kim, and H. Yan, Adv. Mater. (Weinheim, Ger.) **15**, 353 (2003).
[18] D. Zhang, Z. Liu, S. Han, C. Li, B. Lei, M. P. Stewart, J. M. Tour, and C. Zhou, Nano Lett. **4**, 2151 (2004); D. P. Norton, Mater. Sci. Eng., R. **43**, 139 (2004).
[19] M. I. Bichurin, V. M. Petrov, and G. Srinivasan, J. Appl. Phys. **92**, 7681 (2002).
[20] M. I. Bichurin, V. M. Petrov, and G. Srinivasan, Phys. Rev. B **68**, 054402 (2003).
[21] J. Tersoff, Y. H. Phang, Z. Zhang, and M. G. Lagally, Phys. Rev. Lett. **75**, 2730 (1995).
[22] B. S. Kwark, A. Erbil, J. D. Budai, M. F. Chisholm, L. A. Boatner, and B. J. Wilkens, Phys. Rev. B **49**, 14865 (1994).
[23] A. C. Schindler, M. F. Gyure, G. D. Simms, D. D. Vvedensky, R. E. Caflisch, C. Connell, and E. Luo, Phys. Rev. B **67**, 075316 (2003).
[24] *Crystal and Solid State Physics*, edited by K.-H. Hellwege and A. M. Springer, Landolt-Börnstein, New Series, Group III, Vol. 4, Pt. B (Springer-Verlag, New York, 1970).
[25] *Piezoelectric Ceramics Materials Properties* (American Piezo Ceramics, Inc., Mackeyville, PA, 1998).
[26] *Physical Acoustics*, edited by W. P. Mason (Academic, New York, 1965), Vol. III, Pt. B.